DEVELOPMENT OF A 3D LASER BALL BAR FOR THE VOLUMETRIC ERROR MEASUREMENT OF MULTI-AXIS MACHINES

Kuang-Chao Fan
Department of Mechanical Engineering
National Taiwan University
Taipei, Taiwan
ROC

Hai Wang
Department of Mechanical Engineering
Ming-Chi Institute of Technology
Taipei, Taiwan
ROC

Fang-Jung Shiou
Department of Mechanical Eng.
National Taiwan University of Science and Technology
Taipei, Taiwan
ROC

Chih-Wei Ke
Silitek Co.
Hsinchu, Taiwan
ROC

ABSTRACT

Conventional techniques for measuring the volumetric errors of Cartesian coordinate machine tools are time-consuming using laser interferometer or step gauges. For multi-axis machines, where the spindle can swing, the volumetric error calibration is more difficult. In this study, a novel 3D laser ball bar (3D-LBB) has been developed for the easy setup and rapid measurement of the tool position relative to the worktable at any working point of multi-axis machines. The instrument makes use of one laser ball bar and two rotary laser encoders to detect the target path in spherical coordination system. The design of the instrument is discussed and the errors attributes are analyzed to enhance its accuracy. Applications to the volumetric error measurement of a robot and a serial-parallel type machine tool have demonstrated the capability of this 3D-LBB with high precision.

INTRODUCTION

Techniques for performing accuracy testing of CNC machine tools can be found in many standards, such as the ISO 230 or ASME B5.54 (1993). Most of the existing linear measurement instruments are one dimensional, such as the laser interferometer or step gauge. For the circular test of 2D motion, as specified in the ISO 230-4 (1998), some instruments have been developed, such as the, double ball bar (DBB) (Bryan; 1982), Contisure (Burdekin; 1992), and the latest laser ball bar (LBB) (Ziegert; 1994, 2000). Although these instruments are capable of 2-axis error measurements, they are still sensitive to one dimension only.

For the measurement of volumetric errors of machine tools, most methods detect 21 component errors and then use Homogeneous Transformation Matrix (HTM) method or kinematic analysis method (Soons; 1992) to derive the spatial errors in off-line mode. Wang (2000) follows the ASME B5.54 standard to measure volumetric errors directly. It employs a laser Doppler displacement meter (LDDM) and a big flat mirror to measure four body diagonals, and assesses volumetric errors using the vector method. It is time saving but only valid to traditional serial type CNC machines. Recent development of Hexapod machine tools has received a great attention due to its flexibility in 5-axis movement (Patel; 1997). However, owing to the spindle swing in pitch and yaw directions, more sensors are needed to make the volumetric motion measurement possible (Parenti; 1999). In practice, however, this equipment is too expensive to be implemented in industry. So far, there are some good Laser tracking systems (LTS) designed in spherical coordinate system,

which can directly detect the 3D motion error (API; 2002). They must be operated in an active way, which needs feedback sensors and servo control to track the moving target in real time. These systems require very fast control system resulting in expensive cost.

A novel design, which integrates the merits of LBB and LTS is proposed in this research for the three dimensional measurements of moving object in real time phase. This system is based on the spherical coordinate principle containing only one precision Laser linear measurement device and two precision Laser rotary encoders in the gimbals base with an extendable ball bar. Such a system can be dragged by any 3D moving target with a magnetic head and freely moved in the space. Three sensors simultaneously record the ball positions and transform into the Cartesian coordinate in real time. Having calibrated by a HP Laser interferometer, the systematic accuracy can be compensated and enhanced to a higher degree. As this system is operated in the passive mode in 3D space, the cost is cheap. It is called the 3D Laser Ball Bar (3D-LBB).

DESIGN PRINCIPLE OF 3DLBB

Structure Design

Fig. 1 illustrates the system configuration of the 3D-LBB. It is constructed in spherical coordinate of which the center of the gimbals mount is the origin (O_r). Mounted onto the gimbals center, an extendable telescoping tube, made of aluminum alloy and hardened in the interior surface, can be designed in two or three sections depending upon the required radial length of motion. Between the inner and outer tubes of a sliding pair, one linear bearing is mounted at the far end of the outer tube and a copper sliding bearing is fixed at the near end of the inner tube to prevent side motion during bar extension.

The movement of the 3D-LBB is generated by the precision end ball, which can be dragged by a magnet socket carried by any moving object. The radial motion (R) of the ball is detected by a small-sized laser linear measurement system, whose beam passes through telescope tubes and reflected back by a reflector at the bar end. A conical stainless steel connecting the reflector and the ball allows wider angle of rotation

between the magnet socket and the ball. The laser linear system is required as small as possible in order to reduce the system weight. This design was, therefore, changed to a compact Laser Doppler Scale (LDS, model 109N, made by Optodyne Co.) with wavelength stability to 0.1 ppm and system accuracy to 1.0 ppm.
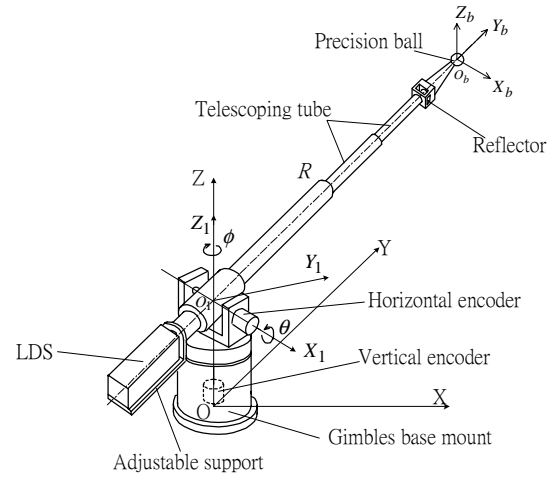
1. THE STRUCTURE OF 3D LASER BALL BAR.

The pitch (θ) and the yaw (ϕ) motions of the bar with respect to the gimbals base are detected by two precision Laser rotary encoders (model K-1, made by Canon Co.) individually. Each encoder has very fine scales of 81,000 ppr. With an additional 16-division interpolator board (model 16-2), the resolution can achieve to one arc-sec.

Coordinate Transformation

To obtain the tool point Cartesian coordinate components, the equations of coordinate measurement can be easily derived as shown in Fig. 2.

$$\left. \begin{aligned} X &= R \cos \theta \sin \varphi \\ Y &= R \cos \theta \cos \varphi \\ Z &= \sin \theta \end{aligned} \right\} \quad (1)$$

where, $R = r_o + r$, r_o is the initial length when bar has no extension and r is the extended length. Fig. 3 shows the picture of the developed prototype 3D-LBB. In order to balance the weight while the telescope tube is extending, a counterweight balancer is mounted onto the

base tube near to the origin. Moreover, for the ease of beam alignment, a four-axis adjustable stage is specially made for laser mounting.

ACCURACY CONSIDERATIONS

As an instrument for the spatial position measurement, the system must be more accurate than the inspected multi-axis machine itself. Error sources, therefore, must be identified and properly calibrated to improve the instrument's system accuracy.
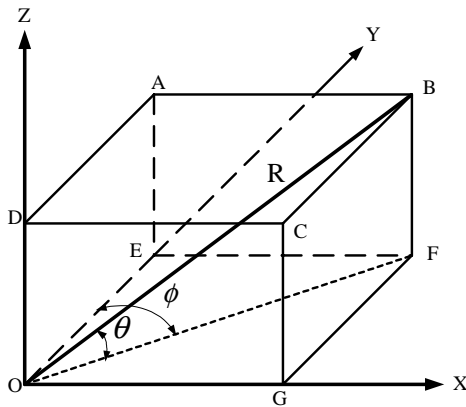
2. SPHERICAL AND CARTESIAN COORDINATES.
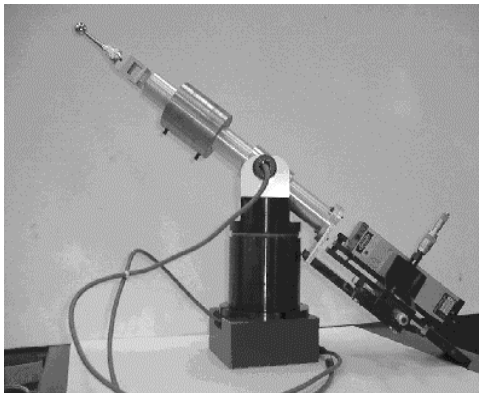
3. THE PROTOTYPE OF 3D-LBB

Clearance Error of the Tubes

As shown in Fig. 4A, under improper fit of the linear bearing a small amount of clearance may generate side motion during the extension of the inner tube.

The angle of rotation can be estimated by $\tan\theta = 2C/L$, where C denotes the clearance and L indicates the bearing length. In this study a copper spacer was particularly designed to give interference fit with the end of the inner tube and precise fit with the outer tube. Under good lubrication the copper spacer can freely slide along the outer tube as a slide bearing. Since, in practice, the linear bearing and tubes has to be selected from the standard items in the shop, a possible clearance even after minor machining still cannot be avoided. The copper spacer, however, can be self-made to assure minimum clearance. Therefore, even to the maximum extension condition, as shown in Fig. 4B, the loose motion of the inner tube must be much smaller than before.
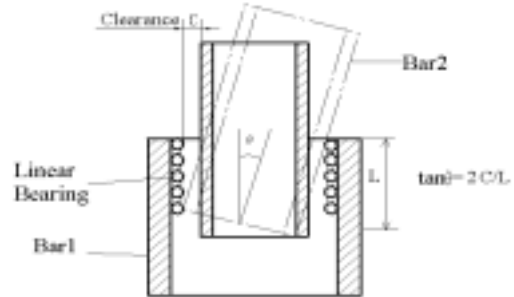
(A)
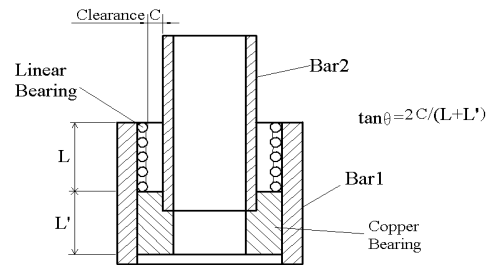
(B)

4. CLEARANCE ERROR: (A) CAUSED BY THE LINEAR BEARING, (B) CORRECTED BY A COPPER BEARING.

Assembly Errors

Geometric assembly errors with constant quantity and direction should be introduced to Eq. (1) in order to modify the measurement inaccuracy. These include the axes perpendicularity, and the axes offset with respective to the origin (O) of the reference

frame XYZ. These errors are illustrated in Figs. 5 to 7 respectively.

As shown in Fig. 5, the perpendicularity error (α) of the θ-axis with respective to the Z axis can be checked by a CMM and computed as

$$\alpha = \arctan \frac{\Delta h}{L} \qquad (2)$$

where, Δh is the difference of the height of two bearing centers and L is the distance between two bearing supports. Another way is to measure the wobble of the rotary disk. Placing a dial gauge at 100mm radial position and rotating the disk a full circle, the height change of the disk surface was found around 0.2μm. Using Eq. (2), the perpendicularity error (α) was about 0.4 arc-sec.

From Fig. 6, the perpendicularity error (β) of the bar with respective to the θ-axis also can be checked by the CMM. The origin O_1 indicates the intersection of the θ-axis and R-axis. From Fig. 7A, in X-Y plane, there is an offset error (a, b) of origin O_1 with respective to origin O of the ϕ-axis. The (a, b) offset could be found by the following procedures:
1. Use the roundness measuring technique to find the offset (a_1, b_1) of the rotary disk center O_o with respect to the rotation center O (refer to Fig. 5).
2. Use CMM to find the offset (a_2, b_2) of the disk center O_o with respect to the origin O_1.
3. Therefore, $a = a_2 - a_1$, $b = b_2 - b_1$.

Then, in Z direction, the deviation c (see Fig. 7B) can be calculated as

$$c = a \tan \alpha + e \cos \alpha \qquad (3)$$

where e is the center offset of the bar-axis with respective to the θ-axis along the Z_1 direction.

Since a, b, c, α, and β are constant assembly errors, these factors must be introduced to the system mechanism, and Eq. (1) has to be modified accordingly. In order to derive the actual measurement equations, two relative coordinate frames are interested, as shown in Fig. 8. The reference frame XYZ is fixed at the base center with the Z-axis denoting the cylindrical base axis. A movable frame $X_1Y_1Z_1$ is assigned at the point O_1 with X_1 parallel to the θ-axis, and Y_1 parallel to the X-Y plane. Eq. (1) can be modified in terms of the homogeneous transformation matrix (HTM)

as below.

$$^oO_b = {}^o[T]_b = [\varphi] \cdot \begin{bmatrix} a \\ b \\ c+h \\ 1 \end{bmatrix} \cdot [\alpha] \cdot [\beta] \cdot [\theta] \cdot [R] \qquad (4)$$

where, ^oO_b denotes the spatial position of ball center with respective to the reference frame XYZ, and h is the actual height of origin O_1 of frame $X_1Y_1Z_1$. Therefore, the actual ball position in space during motion can be calculated with the following equation Eq. (5).
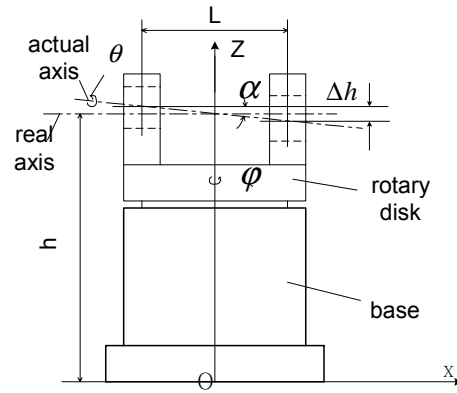
5. SQUARENESS ERROR OF θ-AXIS TO Z-AXIS.
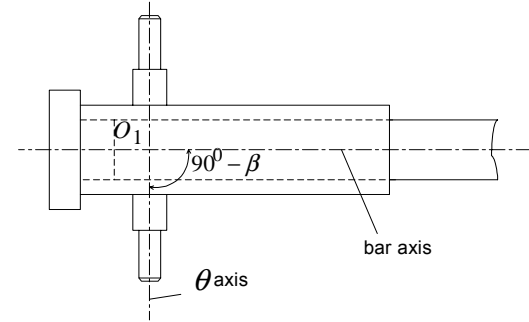
6. SQUARENESS ERROR OF THE θ-AXIS.

$$X = \begin{pmatrix} (\cos \varphi \cos \alpha \sin \beta + \sin \varphi \cos \beta)\cos \theta \\ + \cos \varphi \sin \alpha \sin \theta \end{pmatrix} R$$
$$+ a \cos \varphi + b \sin \varphi$$
$$Y = \begin{pmatrix} (-\sin \varphi \cos \alpha \sin \beta + \cos \varphi \cos \beta)\cos \theta \\ - \sin \varphi \sin \alpha \sin \theta \end{pmatrix} R \qquad (5)$$
$$- a \sin \varphi + b \cos \varphi$$
$$Z = (-\sin \alpha \sin \beta \cos \theta + \cos \alpha \sin \theta)R + c + h$$
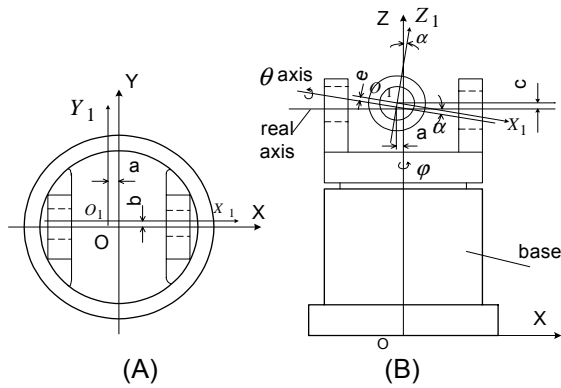
7. THE ECCENTRICITY OF ORIGIN O_1.

Elastic Deformation

Elastic deformation due to the moving bar center and dragging force at the ball is also the essential factor causing the measurement inaccuracy. In this instrument, a balance sleeve was added to effectively reduce the deformation, as shown in Fig. 3. The location and the weight of the balancer are determined such that, at no magnetic drag, when the bar is extended to the half of the total length it reaches to the equilibrium condition. Experiments showed that while the bar is extended to its full length or retracted to its shortest length the small net force variation can be easily absorbed by the magnetic socket.
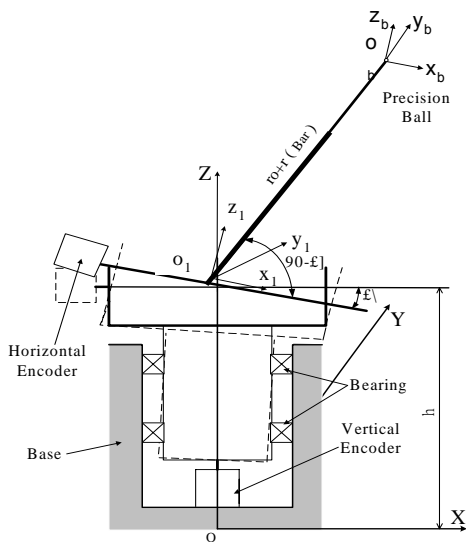
8. STRUCTURAL ASSEMBLY ERRORS.

SYSTEM ACCURACY CALIBRATION

In addition to the geometric errors by assembly and the elastic deformation as described in the above section, there are also other systematic errors, which affect the accuracy of measured R, ϕ and θ data, such as the friction, laser stability and misalignment, clearances of fits, and sensor errors. Therefore, the accuracy calibration of the developed 3D-LBB is necessary. In addition, with the error compensation scheme the system accuracy can be significantly enhanced.

Calibration of the R Axis

As shown in Fig. 9, a HP 5528A laser interferometer was used to compare with the reading of the LDS (not shown in the figure). The 3D-LBB was mounted onto the side table of a table type CMM. Calibrated results are shown in Fig. 10A. Since the error has an obvious tendency and repeatability, the R errors can be compensated by the best fitting line. The modified R reading is expressed by Eq. (6). As shown in Fig. 10B, after compensation, positioning errors of the LDS can be maintained within ± 0.3 μm.

$$R_{\mathrm{mod}} = R_r - 4 \times 10^{-6} R_r - 0.0003 \quad (6)$$

where R_{mod} is the modified R_r value, which is the direct reading from LDS.
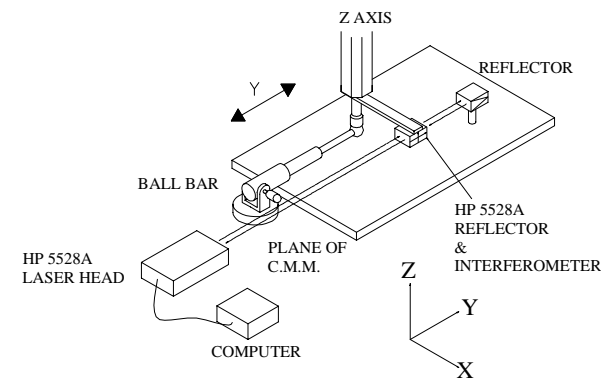
9. SET-UP FOR R ACCURACY CALIBRATION.
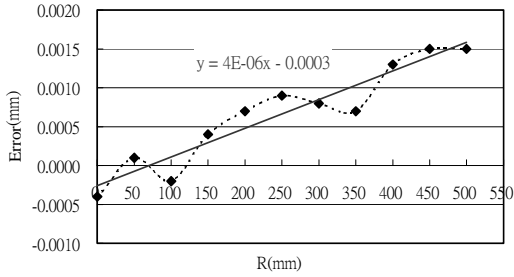
(A)
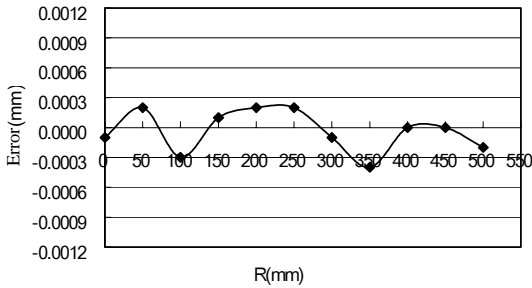
(B)

10. CALIBRATED *R* LINEAR ERRORS: (A) RESULTS; (B) RESIDUAL ERRORS.

Calibration of the ϕ Axis

In this experiment, the bar was carefully aligned to parallel with the X-Y plane and directed to the Y-axis of a table type machine tool, as shown in Fig. 11A. The LBB was mounted on the moving table. During the table moving in the X direction and recorded by a HP 5528A, the ϕ angle changes in trigonometric relationship, as shown in Fig. 11B and expressed by Eq. (8).

$$\phi_i = \arccos\left(\frac{R_0^2 + R_i^2 - X_i^2}{2R_0 R_i}\right) \qquad (7)$$

$$\Delta\phi_i = \phi_{ir} - \phi_i$$

where ϕ_i is the nominal angle at the *ith* position, ϕ_{ir} is the actual readout from vertical encoder.

The calibrated ϕ_i errors can be expressed by Eq. (8). After correction, the ϕ errors can be maintained within around ±1 arc-sec, as shown in Fig. 12.

$$\phi_{\mathrm{mod}} = \phi_r - \left(-4\times10^{-5}\phi_r - 23.818\right) \qquad (8)$$

where ϕ_{mod} is defined as the modified value, and ϕ_r is the readout from the vertical encoder.

(A)

(B)
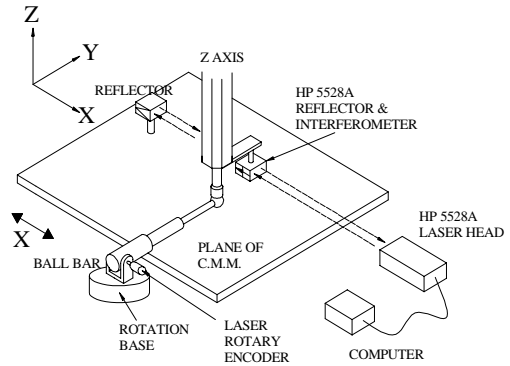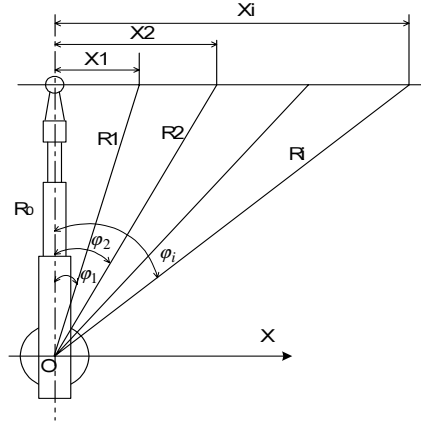
11. (A) SET-UP FOR ϕ CALIBRATION; (B) PRINCIPLE OF CALIBRATION.
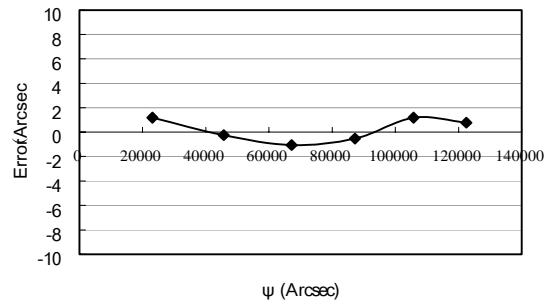
12. CALIBRATED ϕ ANGULAR ERRORS.

Calibration of the θ Axis

The setup and the principle of calibration are similar to Fig. 11 except the laser beam is bent to the spindle direction. With proper alignment, the bar rotates only around the θ-axis. The errors can be found by comparing the θ readouts from the horizontal encoder with reading values of Zi from HP and Ri from LDS, and calculated using Eq. (9). Error correction is done by Eq. (10). Residual errors are about ± 1.6 arc-sec, as shown in Fig. 13.

$$\theta_i = \arccos\left(\frac{R_0^2 + R_i^2 - Z_i^2}{2R_0R_i}\right) \qquad (9)$$

$$\Delta\theta_i = \theta_{ir} - \theta_i$$

where θ_i is defined as an accurate angle and θ_{ir} is the readout from vertical encoder.

$$\theta_{\mathrm{mod}} = \theta_r - \left(-0.0038\times10^{-5}\theta_r - 3.1053\right) \quad (10)$$

where, θ_{mod} is the modified value and θ_r is the readout of the horizontal encoder.
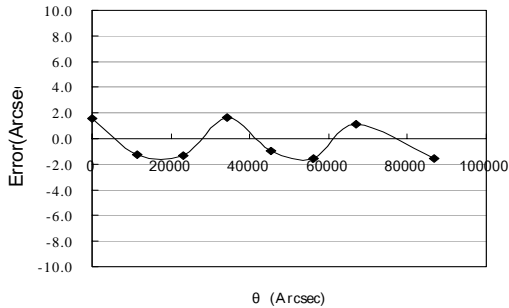
13. CALIBRATED θ ANGULAR ERRORS

Compensated 3D-LBB Errors

After correction of the errors, the measurement accuracy of this instrument is significantly improved, as listed in Table 1.

Table 1: Summary of 3DLBB system accuracy

Coordinate parameters	Range	Accuracy
R	500 mm	± 0.3 μm
ϕ	35 degree	± 1.15 arc-sec
θ	25 degree	± 1.6 arc-sec

APPLICATIONS

Volumetric Error Measurement of a Serial-parallel Type Machine Tool

The experimental setup is shown in Fig.14. The base of the 3D Laser Ball Bar is fixed on the X-Y table. The end ball is mounted at the spindle end by a magnetic socket with three points contact. The machine tool is of a serial-parallel type consisting of a 3-dof parallel spindle platform with two angular orientations and one linear motion in Z-axis, and a conventional X-Y table, which carries the workpiece. Spindle is assembled in the platform, which is connected to three constant length struts by means of ball joints, which are equally spaced at 120 degrees. Giving commands to change two angular orientations of the spindle platform, the tool tip spatial positions could be measured by the 3D Laser Ball Bar. Partial experimental results of volumetric errors are plotted in Fig. 15.
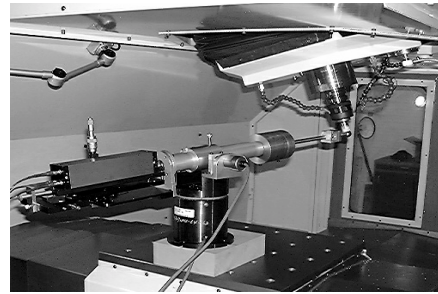
14. SET-UP FOR ACCURACY CHECK OF A SERIAL-PARALLEL MACHINE TOOL.
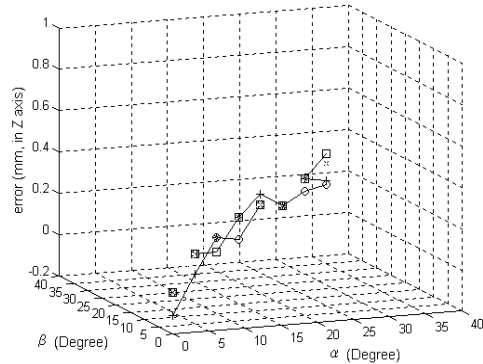
15. DIAGONAL POSITIONING ERROR PLOT.

Robot Spatial Position Error Measurement

According to guideline for robot spatial path

position error calibration (ISO 9283; 1990), the measuring sequence of a standard spatial paths P1→P2→P3→P4→P5→P1 is illustrated in Fig. 16.
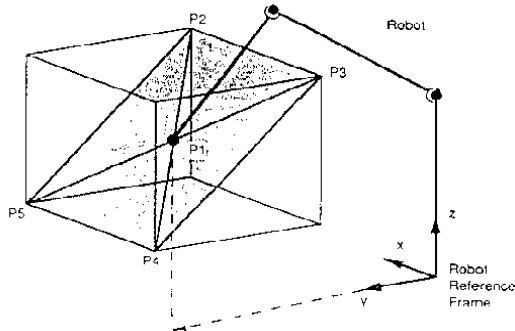
16. SPATIAL PATH FOR ROBOT CALIBRATION.
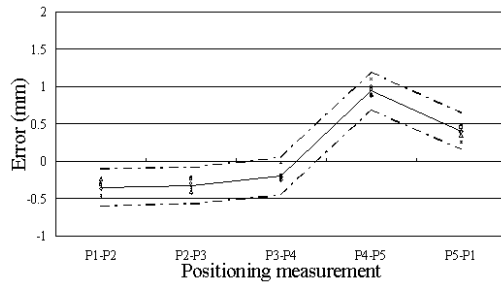
17. RESULTS OF A ROBOT CALIBRATION.

Experimental results are shown in Fig. 17. The repeatability (6 σ) of spatial position errors of the investigated robot is about 0.08 ~ 0.085 mm, which meet general requirements. The maximum spatial position error is about 1mm that implies this robot is only suitable for rugged work.

CONCLUSIONS

A novel 3DLBB system was developed for measuring the volumetric error of multi-axis machines. Its accuracies in $\delta_R = \pm 0.3 \mu m$, $\delta_\phi = \pm 1.15 arc\sec$ and $\delta\theta = \pm 1.6 arc\sec$ were determined by identifying and compensating the possible error sources. In additional to the spatial position measurements, this instrument also can be used to check other kinds of errors in machine tool metrology, such as circular test, straightness and spindle drift etc.

REFERENCES

API Co., (2002), "Laser Tracking System," Internet Access http://www.apisensor.com.

ASME. B5. 54, (1993), "Methods for Performance Evaluation of Computer Numerically Controlled Machining Centers," Version 1.0.

Bryan, J. B., (1982), "A Simple Method for Testing Measuring Machines and Machine Tools," *Precision Engineering*, Vol. 4, No2.

Burdekin, M., and W. Jywe, (1992), "Optimising the Contouring Accuracy of CNC Machines using the Contisure System," *Proc. of the 29th Int. MATADOR Conf.*

ISO 230-4, (1998), Acceptance Code for Machine Tools, Part 4 : Circular Measurements, International Standard.

ISO 9283, (1990), "Manipulating Industrial Robots".

Parenti, V., and R. D. Gregorio, (1999), "Determination of the Actual Configuration of the General Stewart Platform Using One Additional Sensor", *J. of Mechanical Design, Trans. ASME*, Vol.121 (1), pp. 21-25.

Patel, A. J., and K. F. Ehmann, (1997), "Volumetric Error Analysis of a Modified Stewart Platform-based Machine Tool," *Annals of the CIRP*, Vol. 46, No.7, pp. 287-290.

Schmitz, T., and J. Ziegert, (2000), "Dynamic Evaluation of Spatial CNC Contouring Accuracy," *Precision Engineering*, Vol. 24, pp. 99-118.

Soons, J.A., F. C. Theuws, and P. H. Schellekens, (1992), "Modeling the Errors of Multi-axis Machines: A General Methodology," *Precision Engineering*, Vol.14, No. 1, pp. 5-19.

Wang, C., (2000), "Laser Vector Measurement Technique for the Determination and Compensation of Volumetric Positioning Errors," Part 1:Basic theory, *American Institute of Physics*, pp. 3933-3937.

Ziegert, J.C., and C.D. Mize, (1994), "The Laser Ball Bar: a New Instrument for Machine Tool Metrology," *Precision Engineering*, Vol. 16, No. 4, pp. 259-267.